



HAL
open science

The special-linear update: An application of differential manifold theory to the update of isochoric plasticity flow rules

D. Hurtado, Laurent Stainier, M. Ortiz

► To cite this version:

D. Hurtado, Laurent Stainier, M. Ortiz. The special-linear update: An application of differential manifold theory to the update of isochoric plasticity flow rules. *International Journal for Numerical Methods in Engineering*, 2014, 97 (4), pp.298-312. 10.1002/nme.4600 . hal-01007376

HAL Id: hal-01007376

<https://hal.science/hal-01007376>

Submitted on 13 Jun 2019

HAL is a multi-disciplinary open access archive for the deposit and dissemination of scientific research documents, whether they are published or not. The documents may come from teaching and research institutions in France or abroad, or from public or private research centers.

L'archive ouverte pluridisciplinaire **HAL**, est destinée au dépôt et à la diffusion de documents scientifiques de niveau recherche, publiés ou non, émanant des établissements d'enseignement et de recherche français ou étrangers, des laboratoires publics ou privés.

The special-linear update: An application of differential manifold theory to the update of isochoric plasticity flow rules

D. E. Hurtado¹, L. Stainier² and M. Ortiz³

¹*Department of Structural and Geotechnical Engineering, Pontificia Universidad Católica de Chile, Santiago, Chile*

²*Institute of Civil and Mechanical Engineering (GeM, UMR 6183 CNRS), École Centrale Nantes, France*

³*Division of Engineering and Applied Science, California Institute of Technology, Pasadena, CA 91125, USA*

The evolution of plastic deformations in metals, governed by incompressible flow rules, has been traditionally solved using the exponential mapping. However, the accurate calculation of the exponential mapping and its tangents may result in computationally demanding schemes in some cases, while common low-order approximations may lead to poor behavior of the constitutive update because of violation of the incompressibility condition. Here, we introduce the special-linear (SL) update for isochoric plasticity, a flow-rule integration scheme based on differential manifolds concepts. The proposed update exactly enforces the plastic incompressibility condition while being first-order accurate and consistent with the flow rule, thus bearing all the desirable properties of the now standard exponential mapping update. In contrast to the exponential-mapping update, we demonstrate that the SL update can drastically reduce the computing time, reaching one order of magnitude speed-ups in the calculation of the update tangents. We demonstrate the applicability of the update by way of simulation of single-crystal plasticity uniaxial loading tests. We anticipate that the SL update will open the way to efficient constitutive updates for the solution of complex multi-scale material models, thus making it a very promising tool for large-scale simulations.

KEY WORDS: plastic flow rule; crystal plasticity; variational constitutive updates; manifold submersion mappings; applied differential geometry

1. INTRODUCTION

The numerical solution of elasto-viscoplastic problems for solids requires the time integration of flow rules for the determination of the evolution of plastic deformations. In particular, for volume-preserving processes such as plastic deformations in metals, it is desirable that the numerical scheme for the time integration of the flow rule or *flow-rule update* satisfies the plastic incompressibility condition exactly. Volume-preserving flow-rule updates based on the exponential mapping date back to Weber and Anand [1], Eterovic and Bathe [2], Simo [3], and Cuitiño and Ortiz [4] for isotropic plasticity and Miehe [5] and Anand and Kothari [6] for crystal plasticity. The evaluation of the exponential mapping has been the subject of considerable research in the past, see [7] for a review. Some common approaches include the Cayley-Hamilton recursion formula [5], the spectral decomposition and Taylor expansion [8], and more recently, Padé approximants [9]. First-order approximation schemes can also be used in order to alleviate the computational expense attendant to the evaluation of the exponential mapping [4, 10, 11]. However, such approximations are not volume-preserving in general [12] and may thus introduce large errors in the stress update [11].

In this work, we introduce a class of consistent volume-preserving flow-rule updates that are entirely *algebraic* and thus eschew costly spectral analysis and transcendental function evaluations such as inevitably required in the evaluation of the exponential mapping. To this end, we begin by recognizing that the natural space of finite plastic deformations \mathbf{F}^P , namely, the special linear (SL) group $SL(n)$, is not a linear space but has the structure of a Lie group [13]. We recall that Lie groups are *smooth manifolds* that have a continuous multiplicative operation defined on them. In the case of plastic deformations, this operation is simply a matrix multiplication. The corresponding Lie algebra may be identified with the linear space of traceless square matrices. Within this framework, processes of plastic deformation $\mathbf{F}^P(t)$ may be regarded as a continuous flow in $SL(n)$, and the objective of update schemes is to generate approximating discrete flows \mathbf{F}_n^P . Within this context, a flow-rule update is a rule for mapping a point $(\mathbf{F}_n^P, \mathbf{L}^P)$ in the tangent bundle of $SL(n)$ to a new point \mathbf{F}_{n+1}^P in $SL(n)$, where \mathbf{F}_n^P is an initial plastic deformation at time t_n , \mathbf{L}^P is a plastic deformation rate, and \mathbf{F}_{n+1}^P is the updated plastic deformation at time $t_{n+1} = t_n + \Delta t$.

Inspired on differential manifolds concepts, we treat the general form of the incompressible flow rule as a manifold rate problem. Manifold rate problems arise in situations where the evolution of a system is structure-preserving, and therefore, the corresponding integration schemes must also be structure-preserving. The numerical solution of evolution problems governed by differential equations on manifolds has been predominantly studied in the context of Lagrangian mechanics, see [14, 15] and references therein. For example, manifold projection methods have been employed for volume-invariant Lagrangian systems [16]. However, to the best of our knowledge, the application of such methods in the context of material modeling and plasticity has not been reported in the literature to date. In the case of incompressible plasticity, we identify the flow rule as a rate equation on the SL manifold and propose an update that exactly preserves the volume of plastic deformations. The computing time of the proposed update is contrasted with the exponential mapping, showing considerable speed-ups in the computation of the update and its tangents.

This paper is organized as follows. Section 2 is concerned with the development of a constitutive update. We start by introducing basic concepts of differential manifold theory and postulate the general manifold rate problem. On the basis of the concepts of submersion and embedding mappings, we construct an update for the numerical solution of the manifold rate problem that preserves certain structures exactly and that is consistent with the governing rate equations. Then, we introduce the flow rule problem in the context of volume-preserving plasticity and show that it conforms to a manifold rate problem to which we can apply the proposed update. The integration of the proposed flow-rule update within the framework of variational constitutive updates. Section 3 addresses the performance of the proposed SL update in comparison with the exponential mapping update. Numerical simulations of the rate-dependent crystal plasticity model of Cuitiño and Ortiz [4] using the proposed update showcase the applicability of the method. Section 4 ends with a discussion on the obtained results and future perspectives.

2. THE SPECIAL LINEAR UPDATE

The present work draws from the field of differential manifolds to construct numerical updates that preserve certain underlying structure, such as volume invariance in the case of isochoric plasticity.

2.1. Differential manifolds concepts

We begin by briefly reviewing some definitions and concepts from differential manifolds theory that are relevant to this work. The interested reader is referred to [17] for a complete account on differential manifolds theory. Let M be a set of points of interest. The local description of general manifolds is provided by charts. A *chart* on a set M is a pair (U, φ) where $U \subset M$ and $\varphi : U \rightarrow \mathbb{R}^n$ are bijections. Thus, charts are local parameterizations of the set U , and $\varphi(m)$ are the *coordinates* of the point $m \in U \subset M$. We further note that the dimension of $\text{image}(\varphi)$ defines the dimension of the manifold. An *atlas* of class C^k , $k \geq 0$ on a set M consists in a collection of charts $\mathcal{A} = \{(U_i, \varphi_i), i \in I\}$ covering all points in the set M such that any two overlapping charts are

compatible, that is, for (U_i, φ_i) and (U_j, φ_j) such that $U_i \cap U_j \neq \emptyset$, and the overlap map $\varphi_j \circ \varphi_i^{-1}$ is of class C^k . Thus, a C^k -differentiable manifold is a set M together with an atlas \mathcal{A} .

Locally, an n -dimensional manifold looks like \mathbb{R}^n , and for purposes that will be evident later, we are interested in characterizing the tangent structure at every point in a manifold. Let M be a C^1 n -dimensional manifold, and let $\mathbf{x} \in M$ be a point of interest. A C^1 -curve on M through \mathbf{x} is a C^1 -map $\xi : (a, b) \rightarrow M$ such that $\mathbf{x} = \xi(c)$ for $c \in (a, b)$. The representative of the curve in a chart (U, φ) containing \mathbf{x} is the curve $\xi_\varphi = \varphi \circ \xi$ in \mathbb{R}^n . Then, two curves ξ_1 and ξ_2 are *tangent* to M at \mathbf{x} if

$$\xi_1(c) = \xi_2(c) = \mathbf{x} \quad \text{and} \quad \left. \frac{d}{dt}(\varphi \circ \xi_1)(t) \right|_{t=c} = \left. \frac{d}{dt}(\varphi \circ \xi_2)(t) \right|_{t=c} = \mathbf{v}, \quad (1)$$

where \mathbf{v} is the *tangent vector* associated to the equivalence class of curves implicitly defined by (1). It can be shown that these definitions do not depend on the chart of choice [17]. Thus, we define the *tangent space* to M at \mathbf{x} as the set of all tangent vectors $\mathbf{v} \in \mathbb{R}^n$ and denote it by $T_{\mathbf{x}}M$. It can also be shown that $T_{\mathbf{x}}M$ is in fact a linear space. The set $TM := \{(\mathbf{x}, \mathbf{u}), \mathbf{x} \in M, \mathbf{u} \in T_{\mathbf{x}}M\}$ is the *tangent bundle*. It can be shown that if M is a C^k -manifold of dimension n ; then, TM is in fact a C^k -manifold of dimension $2n$ [17]. A *vector field* is a mapping $\mathbf{u} : M \rightarrow TM$ that assigns a vector $\mathbf{u}(\mathbf{x})$ to a point $\mathbf{x} \in M$.

Consider now the map $f : M \rightarrow N$ of a manifold M to a manifold N . Then, f is a C^k -map if its representation in local coordinates on M , and N is a C^k mapping in the classical way. The *derivative* of a differentiable map is defined as the linear map $T_{\mathbf{x}}f : T_{\mathbf{x}}M \rightarrow T_{f(\mathbf{x})}N$ such that for $\mathbf{v} \in T_{\mathbf{x}}M$

$$T_{\mathbf{x}}f \cdot \mathbf{v} = \left. \frac{d}{dt} f(\xi(t)) \right|_{t=c}, \quad (2)$$

where the curve ξ satisfies (1).

A subset $S \subset M$ modeled on \mathbb{R}^n is a *submanifold* of M if there exists an atlas \mathcal{A} of M such that, for all $(U, \varphi) \in \mathcal{A}$ such that $U \cap S \neq \emptyset$ we have that $\varphi(U \cap S) = \varphi(U) \cap \mathbb{R}^m$ for some $m \leq \dim(M)$. Certain mappings can be used to construct submanifolds. A mapping $f : M \rightarrow N$ is a C^k -*diffeomorphism* if it is bijective and f and f^{-1} are both C^k . An *immersion* is a mapping $f : M \rightarrow N$ such that $T_{\mathbf{x}}f$ is everywhere injective or, equivalently, if $T_{\mathbf{x}}f$ has constant rank equal to the dimension of M . An *embedding* is an immersion that is *diffeomorphic* to its image, with the consequence that $f(M)$ is a submanifold of N . A C^k mapping $g : M \rightarrow N$ is a *submersion* if $T_{\mathbf{x}}g$ is everywhere surjective or, equivalently, if $T_{\mathbf{x}}g$ has constant rank equal to the dimension of n .

2.2. Manifold updates and the manifold rate problem

A situation that arises in practice concerns the need to update a point \mathbf{x} on a manifold M along a vector $\mathbf{u} \in T_{\mathbf{x}}M$. Specifically, by a *linear update*, we understand a mapping $\text{upd}_{\mathbf{x}} : T_{\mathbf{x}}M \rightarrow M$ such that the following *consistency conditions* hold

$$\text{upd}_{\mathbf{x}}(0) = \mathbf{x} \quad (3a)$$

$$T_0 \text{upd}_{\mathbf{x}} = \text{id}, \quad (3b)$$

where id is the identity operator. In Euclidean space E^n , consistency conditions (3) imply that a linear update is necessarily of the form

$$\text{upd}_{\mathbf{x}}(\mathbf{u}) = \mathbf{x} + \mathbf{u}, \quad (4)$$

as expected. For a general manifold, conditions (3) require that updates have the structure (4) locally. In particular, the zeroth-order consistency condition (3a) simply states that updates must reduce to the identity for the zero tangent vector. An alternative expression for the first-order consistency condition (3b) is

$$\left. \frac{d}{dt} \text{upd}_x(\boldsymbol{\xi}(t)) \right|_{t=0} = \mathbf{u} \quad (5)$$

which must hold for all curves $\boldsymbol{\xi}$ such that $\boldsymbol{\xi}(0) = \mathbf{x}$ with tangent vector \mathbf{u} at \mathbf{x} .

A particularly important type of update may be formulated in the case of manifolds embedded in Euclidean space by using the embedding mapping to reduce the update to the form (4). Thus, if $f : M \rightarrow E^n$ is an embedding into the Euclidean space and $g : E^n \rightarrow M$ is a submersion such that

$$(g \circ f)(\mathbf{x}) = \mathbf{x} \quad \forall \mathbf{x} \in M \quad (6)$$

then, a simple update is given by

$$\text{upd}_x(\mathbf{u}) = g(f(\mathbf{x}) + T_x f \cdot \mathbf{u}). \quad (7)$$

We readily verify that for this class of updates, consistency conditions hold, namely

$$\text{upd}_x(\mathbf{0}) = g(f(\mathbf{x})) = \mathbf{x} \quad (8a)$$

$$T_0 \text{upd}_x = T_{f(\mathbf{x})} g \cdot T_x f = \text{id} \quad \text{over } T_x M, \quad (8b)$$

where the chain rule has been used in (8b).

We now illustrate the use of updates in the context of explicit calculations for the solution of differential equations on manifolds. We begin by considering the *manifold rate problem*

$$\dot{\mathbf{x}}(t) = \mathbf{u}(\mathbf{x}(t)), \quad (9a)$$

$$\mathbf{x}(0) = \mathbf{x}_0, \quad (9b)$$

where $\mathbf{x}_0 \in M$ is a point on the manifold, $\mathbf{x}(t)$ is a curve, *the integral curve*, over the manifold M , and $\mathbf{u} \in TM$ is a vector field. Suppose that an approximation to the solution \mathbf{x}_k is known at time t_k , $k \in \mathbb{N}$ and that we wish to determine the next approximation \mathbf{x}_{k+1} to the state of the system at time $t_{k+1} = t_k + h$. A simple scheme for marching forward in time is the forward-Euler scheme

$$\mathbf{u}_k = \mathbf{u}(\mathbf{x}_k) \quad (10a)$$

$$\mathbf{x}_{k+1} = \text{upd}_{\mathbf{x}_k}(h \mathbf{u}_k) \quad (10b)$$

where $\text{upd}_{\mathbf{x}_k} : T_{\mathbf{x}_k} M \rightarrow M$ is an update over the manifold M . In this simple scheme, (10a) evaluates the rate \mathbf{u}_k at time t_k , and then, it is left to the update to march forward from \mathbf{x}_k at the rate \mathbf{u}_k over the interval of time h . We verify that, by virtue of the consistency conditions (3)

$$\left. \frac{d}{dh} \mathbf{x}_{k+1} \right|_{h=0} = T_0 \text{upd}_x(\mathbf{u}_k) = \mathbf{u}_k, \quad (11)$$

and the scheme (10) is indeed consistent with the rate problem defined by (9). Moreover, the scheme is first-order accurate, see Appendix A. In the particular case of embedded manifolds and the update (7), (10b) becomes

$$\mathbf{x}_{k+1} = g(f(\mathbf{x}_k) + h T_{\mathbf{x}_k} f \cdot \mathbf{u}_k). \quad (12)$$

In this case, the time-stepping scheme reduces to embed \mathbf{x}_k into E^n , applying the forward-Euler scheme in E^n , and finally projecting back to the manifold.

2.3. Flow rules in volume-preserving metal plasticity

In phenomenological rate-dependent plasticity theory, the time-evolution of plastic deformations and internal variables is governed by rate equations. For present purposes, it suffices to consider the kinematics of plastic deformation. The interested reader is referred to [18, 19] for a comprehensive review of plasticity theories.

We start by considering a Lagrangian finite-kinematics framework, where the body in the undeformed configuration occupies a domain $B \in \mathbb{R}^3$. The deformation mapping $\varphi : B \times [0, t_f] \rightarrow \mathbb{R}^3$

maps point in the undeformed configuration into the current or deformed configuration. The deformation gradient $\mathbf{F} := \nabla_0 \varphi$ measures variations of φ in the vicinity of a point $\mathbf{X} \in B$, describing local rotation and stretch. In large-deformation plasticity, it is customary to assume a multiplicative decomposition [20, 21] of the form

$$\mathbf{F} = \mathbf{F}^e \mathbf{F}^p, \quad (13)$$

where \mathbf{F}^e and \mathbf{F}^p are the elastic and plastic deformation gradients, respectively. Following an internal variable formalism [22, 23], the local state of a solid is determined by the deformation gradient \mathbf{F} , the plastic deformation gradient \mathbf{F}^p , and a set of internal variables $\boldsymbol{\xi} \in \mathbb{R}^N$. Due to the phenomenological nature of plasticity theories, the physical meaning of the internal variables $\boldsymbol{\xi}$ depends on the particular material under consideration. It is then classical to postulate the existence of a Helmholtz free energy potential or state function $A(\mathbf{F}, \mathbf{F}^p, \boldsymbol{\xi})$. Assuming that work-hardening and lattice distortion are uncoupled phenomena, the free energy then takes the form

$$A(\mathbf{F}, \mathbf{F}^p, \boldsymbol{\xi}) = W^e(\mathbf{F}^e) + W^p(\mathbf{F}^p, \boldsymbol{\xi}) = W^e(\mathbf{F} \mathbf{F}^{p-1}) + W^p(\mathbf{F}^p, \boldsymbol{\xi}) \quad (14)$$

where W^e is the elastic deformation energy and W^p is the plastic stored energy that determines the plastic hardening of the material. In local equilibrium state, the first Piola-Kirchhoff stress tensor is obtained from the free energy density as

$$\mathbf{P} = \frac{\partial A}{\partial \mathbf{F}}, \quad (15)$$

which clearly depends on the material *local state* represented by $(\mathbf{F}, \mathbf{F}^p, \boldsymbol{\xi})$. The thermodynamic forces conjugate to the internal variables or *driving forces* derive from the free energy and take the form

$$\mathbf{Y} = -\frac{\partial A}{\partial \boldsymbol{\xi}}. \quad (16)$$

The time-evolution of internal variables may then be assumed to depend only on the conjugate driving force, resulting in kinetic equations of the general form

$$\dot{\boldsymbol{\xi}} = \mathbf{f}(\mathbf{Y}) \quad (17)$$

where $[\dot{\circ}] = \frac{\partial[\circ]}{\partial t}$ denotes partial differentiation with respect to time. In order to automatically fulfill the second principle of thermodynamics (non-negative dissipation), it is customary to rewrite the earlier kinetic equations through the use of a convex dissipation potential $\psi^*(\mathbf{Y})$, such that

$$\dot{\boldsymbol{\xi}} = \frac{\partial \psi^*}{\partial \mathbf{Y}}. \quad (18)$$

A conjugate dissipation potential $\psi(\dot{\boldsymbol{\xi}})$ can be built by a Legendre transform, with

$$\psi(\dot{\boldsymbol{\xi}}) = \sup_{\mathbf{Y}} [\mathbf{Y} \cdot \dot{\boldsymbol{\xi}} - \psi^*(\mathbf{Y})]. \quad (19)$$

Kinetic equations can then be written under the alternative form

$$\mathbf{Y} = \frac{\partial \psi}{\partial \dot{\boldsymbol{\xi}}} \quad \text{or} \quad \frac{\partial A}{\partial \boldsymbol{\xi}} + \frac{\partial \psi}{\partial \dot{\boldsymbol{\xi}}} = 0. \quad (20)$$

In addition, the time evolution of the plastic deformation gradient is defined by a flow rule of the general form [24]

$$\mathbf{L}^p = \dot{\mathbf{F}}^p \mathbf{F}^{p-1} = \dot{\boldsymbol{\xi}} \mathbf{M}, \quad (21)$$

where \mathbf{M} is a tensor imposing constraints on the instantaneous direction of plastic deformation, which depends on the particular plasticity model chosen. Examples are provided in [24]. Considering the flow rule as a constraint between the plastic deformation gradient \mathbf{F}^P and the internal variables $\boldsymbol{\xi}$, driving forces \mathbf{Y} defined by (16) can be expressed as

$$\mathbf{Y} = \mathbf{M} \mathbf{T} \mathbf{F}^{P T} - \frac{\partial W^P}{\partial \boldsymbol{\xi}} \quad (22)$$

where the stress tensor \mathbf{T} , conjugate to \mathbf{F}^P , is defined by

$$\mathbf{T} = -\frac{\partial A}{\partial \mathbf{F}^P} = \mathbf{F}^{e T} \mathbf{P} - \frac{\partial W^P}{\partial \mathbf{F}^P}. \quad (23)$$

In this equation, the last term represents a backstress tensor, denoting the presence of kinematic hardening.

Working at the scale of single crystals, the flow rule is based on direct observations of the deformation patterns found in crystalline materials, where plastic deformation occurs along well-defined sets of crystallographic planes, defined by their normals \mathbf{m}^α , and slip directions s^α , $\alpha = 1, \dots, N$, taking the form

$$\mathbf{M} = \{s^1 \otimes \mathbf{m}^1, \dots, s^N \otimes \mathbf{m}^N\}. \quad (24)$$

It bears emphasis that, in this case as well as for macroscopic models of plasticity (Tresca and von Mises) considered in [24], it results from these kinematic assumptions on the direction of plastic velocity gradient that plastic deformations are volume-preserving. Indeed,

$$\frac{\partial}{\partial t} \det(\mathbf{F}^P) = \det(\mathbf{F}^P) \text{trace}(\dot{\mathbf{F}}^P \mathbf{F}^{P-1}) = \det(\mathbf{F}^P) \text{trace}(\dot{\boldsymbol{\xi}} \mathbf{M}) = 0 \quad (25)$$

where the last equality results from the traceless character of the tensor \mathbf{M} . We further note that the zero-trace condition is independent of the internal state $\boldsymbol{\xi}$. Assuming no plastic deformation is present initially in the solid we have

$$\mathbf{F}^P|_{t=0} = \mathbf{I}, \quad (26)$$

which together with (25) implies that $\det \mathbf{F}^P(\mathbf{X}, t) = 1$, that is, $\mathbf{F}^P(\mathbf{X}, t)$ belongs to the *special linear group*, which is denoted by $SL(3)$. Recall that the general linear group $GL(3) := \{\mathbf{F} \in \mathbb{R}^{3 \times 3}, \det \mathbf{F} \neq 0\}$ is a smooth manifold, see [17]. It follows that $SL(3)$ is a submanifold of $GL(3)$, and therefore a manifold itself. We thus conclude that the ordinary differential equation (21) together with the initial condition (26) define a rate problem on $SL(3)$.

2.4. Variational constitutive updates

The numerical integration of elasto-viscoplastic constitutive relations can be performed by recourse to variational constitutive updates, see [24] for a full account of the theory. In this section, we recall the relevant definitions and results, and show how the proposed SL update can be incorporated into the variational constitutive update framework.

The determination of the plastic internal variables $(\mathbf{F}^P, \boldsymbol{\xi})$ requires the time integration of the kinetic equations and flow rule. For such purposes, consider the discretization of the evolution problem into a finite number of time intervals $[t_n, t_{n+1}]$, $n \in \mathbb{N}$. Then, the time integration of (18) is equivalent to solving the minimization problem

$$W_n(\mathbf{F}_{n+1}) = \min_{\boldsymbol{\xi}_{n+1}} \left\{ A(\mathbf{F}_{n+1}, \mathbf{F}_{n+1}^P, \boldsymbol{\xi}_{n+1}) - A_n + \Delta t \left(\frac{\boldsymbol{\xi}_{n+1} - \boldsymbol{\xi}_n}{\Delta t} \right) \right\} \quad (27)$$

where A_n is the free energy density evaluated at $t = t_n$ and considered constant for all purposes and $W_n(\mathbf{F}_{n+1})$ is known as the incremental energy density for time step n . The minimization problem that defines the incremental energy density in (27) can be shown to be equivalent to the time integration of the kinetic equations using an implicit backward-Euler scheme. In writing (27),

one implicitly assumes that the relation between \mathbf{F}_{n+1}^p and ξ_{n+1} , which is constrained by (21), is known. In accordance to (25) and (26), this relation should also ensure that $\det \mathbf{F}_{n+1}^p = 1$. Volume-preserving flow-rule updates based on the exponential mapping have been used extensively for this purpose [1–6, 24]

$$\mathbf{F}_{n+1}^p = \exp [(\xi_{n+1} - \xi_n) \mathbf{M}] \mathbf{F}_n^p. \quad (28)$$

As mentioned before, practical computation of this exponential mapping is typically costly and potentially suffers from a lack of robustness [7, 8].

We now show how to apply the concept of manifold updates to the integration of the incompressible plastic flow rule. We consider the mapping $g : GL(3) \rightarrow SL(3)$ defined by

$$g(\mathbf{F}) = (\det \mathbf{F})^{-\frac{1}{3}} \mathbf{F} \quad (29)$$

and note that g is a submersion mapping, see Appendix B. Moreover, consider the inclusion map $f : SL(3) \hookrightarrow GL(3)$, which is also an embedding [17]. Thus, we define the SL update by considering the general manifold update defined in (7) using the submersion and embedding mappings just defined for this case. Consider the time interval $[t_n, t_{n+1}]$ with time step $\Delta t = t_{n+1} - t_n$, and assume \mathbf{F}_n^p and ξ_n are known from previous calculations. We approximate the internal variable rate by the finite difference scheme

$$\dot{\xi} \approx \frac{\xi_{n+1} - \xi_n}{\Delta t}. \quad (30)$$

Then, for a given value of ξ_{n+1} , the SL update reads

$$\mathbf{F}_{n+1}^p(\xi_{n+1}) = \text{upd}_{\mathbf{F}_n^p} [(\xi_{n+1} - \xi_n) \mathbf{M} \mathbf{F}_n^p], \quad (31)$$

which, in view of (12) and (29) takes the form

$$\mathbf{F}_{n+1}^p(\xi_{n+1}) = (\det \{ \mathbf{F}_n^p + (\xi_{n+1} - \xi_n) \mathbf{M} \mathbf{F}_n^p \})^{-\frac{1}{3}} [\mathbf{F}_n^p + (\xi_{n+1} - \xi_n) \mathbf{M} \mathbf{F}_n^p], \quad (32)$$

where we have used the fact that $T_{\mathbf{F}_n^p} f = \mathbf{I}$ for all $\mathbf{F}_n^p \in SL(3)$ because f is an inclusion map.

We note that, from the definition of manifold updates, it follows that the SL update exactly preserves the incompressibility condition while being consistent with the governing differential equation.

For the case of incompressible materials conforming to flow rules of the form (21), where $\dot{\xi} \mathbf{M}$ is a traceless tensor, the SL update proposed in (31) thus delivers a volume-preserving relation, in fact, a function, between \mathbf{F}_{n+1}^p and ξ_{n+1} , which can be used in the solution of (27). The minimization problem in (27) is most effectively solved using gradient descent methods, typically in the form of a Newton-Raphson scheme. To this end, the first and second tangents of (31) are needed. The expression for such tangents has been included in Appendix B.

2.5. Consistency

In this section, we demonstrate the consistency of variational constitutive update (27) when using the SL update (31). To this end, let us write the Euler-Lagrange equation expressing stationarity with respect to ξ_{n+1} :

$$\frac{\partial A}{\partial \mathbf{F}^p}(\mathbf{F}, \mathbf{F}_{n+1}^p, \xi_{n+1}) : \frac{\partial \mathbf{F}_{n+1}^p}{\partial \xi_{n+1}} + \frac{\partial A}{\partial \xi}(\mathbf{F}, \mathbf{F}_{n+1}^p, \xi_{n+1}) + \frac{\partial \psi}{\partial \dot{\xi}} \left(\frac{\xi_{n+1} - \xi_n}{\Delta t} \right) = 0. \quad (33)$$

Using (14) and (23), this stationarity equation can be rewritten as

$$- \mathbf{T}_{n+1} : \frac{\partial \mathbf{F}_{n+1}^p}{\partial \xi_{n+1}} + \frac{\partial W^p}{\partial \xi}(\mathbf{F}_{n+1}^p, \xi_{n+1}) + \frac{\partial \psi}{\partial \dot{\xi}} \left(\frac{\xi_{n+1} - \xi_n}{\Delta t} \right) = 0. \quad (34)$$

Solving this nonlinear equation for ξ_{n+1} (with (31)) yields updated values of internal variables. The incremental plastic update (31) can alternatively be expressed as

$$\mathbf{F}_{n+1}^p = g\left(\hat{\mathbf{F}}_{n+1}^p\right) \quad \text{where} \quad \hat{\mathbf{F}}_{n+1}^p = f\left(\mathbf{F}_n^p\right) + \left(\xi_{n+1} - \xi_n\right) T_{F_n^p} f \cdot \mathbf{M} \mathbf{F}_n^p. \quad (35)$$

Variations of the plastic deformation gradient with respect to internal variables then writes

$$\frac{\partial \mathbf{F}_{n+1}^p}{\partial \xi_{n+1}} = T_{\hat{\mathbf{F}}_{n+1}^p} g \cdot T_{F_n^p} f \cdot \mathbf{M} \mathbf{F}_n^p \quad (36)$$

where we have used the chain rule. Noting that

$$\lim_{\xi_{n+1} \rightarrow \xi_n} \hat{\mathbf{F}}_{n+1}^p = f\left(\mathbf{F}_n^p\right) \quad (37)$$

we can thus write

$$\lim_{\xi_{n+1} \rightarrow \xi_n} \frac{\partial \mathbf{F}_{n+1}^p}{\partial \xi_{n+1}} = T_{f(F_n^p)} g \cdot T_{F_n^p} f \cdot \mathbf{M} \mathbf{F}_n^p = \mathbf{M} \mathbf{F}_n^p \quad (38)$$

where we have used (6). Then, for vanishing increment size, stationarity equation (34) tends to

$$-Y_n + \frac{\partial \psi}{\partial \xi}(\xi_n) = 0 \quad (39)$$

which is consistent with the continuous kinetic equations (20).

We end this section by noting that the first Piola-Kirchhoff stress is then obtained as

$$\mathbf{P}_{n+1} = \frac{\partial W_n}{\partial \mathbf{F}_{n+1}}. \quad (40)$$

This result is easily obtained by considering the stationarity condition (33), as shown in [24]. The consistent tangents are also of critical importance in implicit approaches (e.g. quasistatic problems). They are readily obtained by

$$\begin{aligned} \mathbf{K} \equiv \frac{\partial \mathbf{P}_{n+1}}{\partial \mathbf{F}_{n+1}} &= \frac{\partial^2 A}{\partial \mathbf{F} \partial \mathbf{F}}\left(\mathbf{F}_{n+1}, \mathbf{F}_{n+1}^p(\xi_{n+1}), \xi_{n+1}\right) \\ &\quad - \frac{\partial^2 J_n}{\partial \mathbf{F} \partial \xi}\left(\mathbf{F}_{n+1}, \xi_{n+1}\right) \cdot \left[\frac{\partial^2 J_n}{\partial \xi \partial \xi}\right]^{-1}\left(\mathbf{F}_{n+1}, \xi_{n+1}\right) \cdot \frac{\partial^2 J_n}{\partial \xi \partial \mathbf{F}}\left(\mathbf{F}_{n+1}, \xi_{n+1}\right) \end{aligned} \quad (41)$$

where the function $J_n(\mathbf{F}, \xi)$ is defined as

$$J_n(\mathbf{F}, \xi) = A(\mathbf{F}, \mathbf{F}_{n+1}^p(\xi), \xi) - A_n + \Delta t \quad \left(\frac{\xi - \xi_n}{\Delta t}\right). \quad (42)$$

Note that in these expressions, we make use of the SL update (31).

3. NUMERICAL SIMULATIONS

To assess the performance and advantages of the SL update over the exponential mapping update, we have carried out numerical exercises to determine the computing time of each method. In all computations of the exponential mapping and its first and second linearizations, we have considered its spectral expansion form, see [8]. To account for the most favorable scenario for the exponential mapping, we have considered randomly generated symmetric traceless matrices, which result in real eigenvalues, thus reducing the computation effort needed in the evaluation of the exponential mapping compared to the case of non-symmetric matrices, see [7]. We have verified that the computation time of the SL update is roughly insensitive to degree of symmetry of the matrix. Figure 1 shows the histogram for the computing-time ratio of the exponential mapping to the SL update, from where

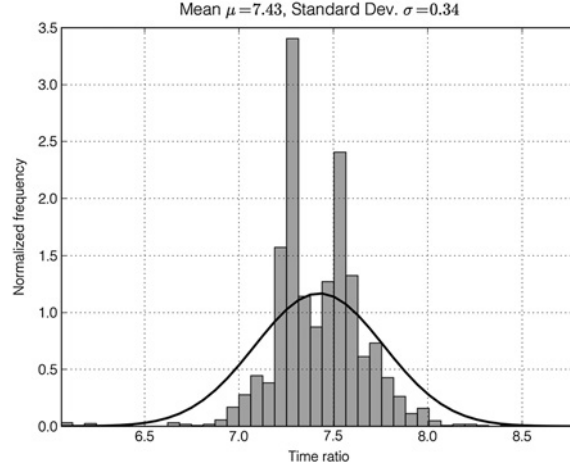


Figure 1. Computing-time ratio of the exponential mapping to the super linear mapping.

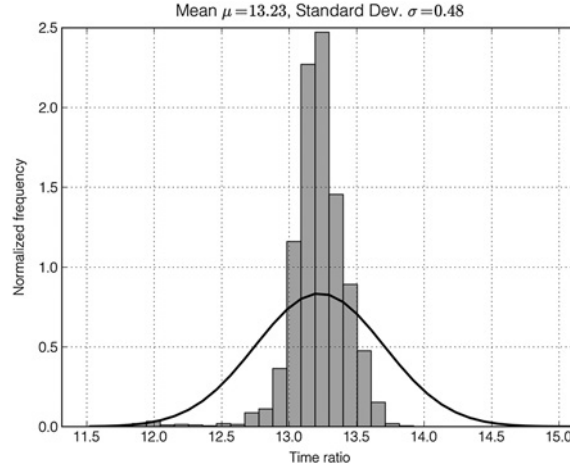


Figure 2. Computing-time ratio of the first linearization of the exponential mapping to the first linearization of the super linear mapping.

we observe that the SL update is, in average, 7.4 times faster than the exponential mapping. We note that the standard deviation in this ratio is relatively small, and therefore, the SL update shows a marked and relatively uniform speedup over the exponential mapping update. Because the first and second linearizations of both mappings are fundamental to the computation of algorithmically consistent tangents and in turn in the solution of Newton-Raphson iterations, we have also assessed the performance of the first and second linearizations of both mappings. Figures 2 and 3 show the computing-time ratio of the SL update to the exponential mapping for the first and second linearizations, respectively. Remarkably, the SL update results in computing times that are, in average, 13.23 and 34.83 times faster than the first and second linearizations of the exponential mapping update, respectively.

To showcase the applicability of the proposed update in the solution of the time integration of constitutive relations of metals, the single crystal plasticity model of Cuitiño and Ortiz [4] has been implemented into the framework of variational constitutive updates using the SL update introduced in (31). In this case, the plastic deformation mapping and internal variables are constrained through the crystallographic flow rule defined by (21) using a kinematic tensor of the form (24). For crystal-plasticity formulations, the internal variables are physically motivated by the slip strain γ^α associated to the α - slip system of the crystal, traditionally denoting the array of such internal

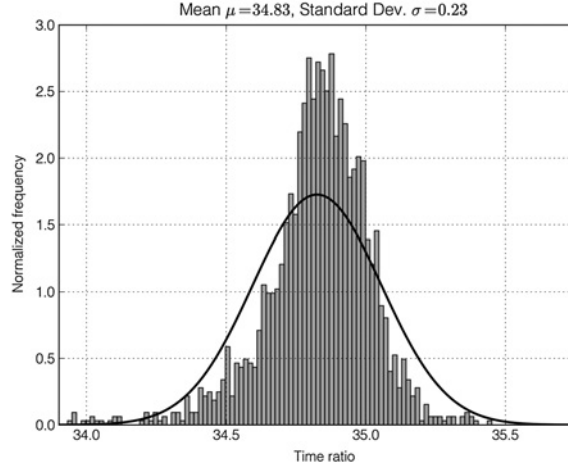


Figure 3. Computing-time ratio of the second linearization of the exponential mapping to the second linearization of the super linear mapping.

variables by $\boldsymbol{\gamma} = \{\gamma^1, \dots, \gamma^N\}$. In the following examples, we have considered copper single crystals with face-centered cubic set of slip systems, see, for example, [4]. The elastic energy density W^e follows a cubic-Hookean model,

$$W^e(\mathbf{F}^e) = \frac{1}{2} \boldsymbol{\varepsilon}^e : \mathbb{C}_{cubic} : \boldsymbol{\varepsilon}^e, \quad (43)$$

where $\boldsymbol{\varepsilon}^e = \frac{1}{2} \log(\mathbf{F}^{eT} \mathbf{F}^e)$ is the Hencky strain tensor and \mathbb{C}_{cubic} is the elasticity tensor with cubic symmetry defined by elastic constants \mathbb{C}_{11} , \mathbb{C}_{12} , and \mathbb{C}_{44} . The dislocation-based hardening model of Cuitiño and Ortiz has been approximated using a quadratic expression suitable for variational constitutive updates [24], leading to a plastic stored energy density of the form

$$W^p(\boldsymbol{\gamma}_{n+1}) = W_n^p + \sum_{\alpha}^N \left(g_n^{\alpha} \Delta \gamma^{\alpha} + \frac{1}{2} \Delta \gamma^{\alpha} \sum_{\beta}^N h_n^{\alpha\beta} \Delta \gamma^{\beta} \right), \quad (44)$$

where $\Delta \gamma^{\alpha} = \gamma_{n+1}^{\alpha} - \gamma_n^{\alpha}$ and the diagonal hardening matrix takes the form

$$h^{\alpha\alpha} = h_c^{\alpha} \left(\frac{g^{\alpha}}{\tau_c^{\alpha}} \right)^3 \left\{ \cosh \left[\left(\frac{\tau_c^{\alpha}}{g^{\alpha}} \right)^2 \right] - 1 \right\}, \quad (45)$$

where

$$h_c^{\alpha} = \frac{\tau_c^{\alpha}}{\gamma_c^{\alpha}}, \quad \tau_c^{\alpha} = \alpha \mu b \sqrt{\pi n^{\alpha}}, \quad \gamma_c^{\alpha} = \frac{b \rho^{\alpha}}{2 \sqrt{n^{\alpha}}} \quad (46)$$

are the characteristic plastic modulus, critical resolved shear stress, and critical slip strain for the slip system α , respectively, and

$$n^{\alpha} = \sum_{\beta}^N a^{\alpha\beta} \rho^{\beta} \quad (47)$$

represents the density of obstacles due to forest dislocations, where the matrix $a^{\alpha\beta}$ is defined by the constants a_0 , a_1 , a_2 , and a_3 , as addressed in [25]. The dislocation density is related to the slip strain by the expression

$$\rho^{\alpha} = \rho_{\text{sat}} \left[1 - \left(1 - \frac{\rho_0}{\rho_{\text{sat}}} \right) \exp(\gamma^{\alpha} / \gamma_{\text{sat}}) \right]. \quad (48)$$

Table I. Material parameters for copper single crystal.

Parameter	Value	Unit
C_{11}	168.4	GPa
C_{12}	121.4	GPa
C_{44}	75.4	GPa
$\dot{\gamma}_0$	1.0	s^{-1}
m	100	
τ_0	2.0	MPa
ρ_0	1.0×10^{10}	m^{-2}
ρ_{sat}	1.0×10^{13}	m^{-2}
γ_{sat}	0.5%	
g^α	2.0	MPa
a_0	8.0×10^{-4}	
a_1	$5.7 a_0$	
a_2	$10.2 a_0$	
a_3	$16.6 a_0$	
α	0.3	
b	2.56×10^{-10}	m
μ	75.4	GPa

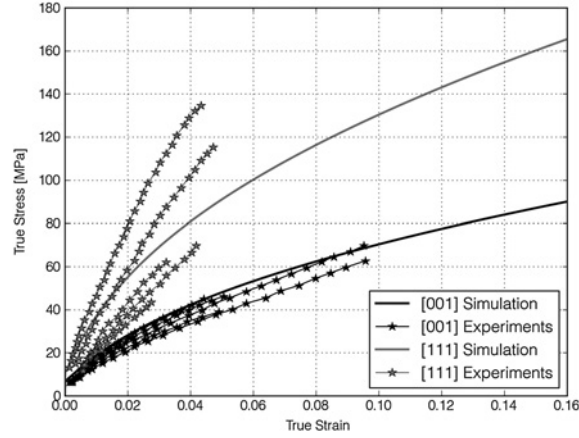


Figure 4. Single-crystal uniaxial tension test: a comparison of simulations and experiments for different loading orientations.

The power-law rate-dependent behavior is incorporated into the single crystal model by the consideration of a convex l.s.c. power-law dissipation potential [24], namely,

$$= \begin{cases} \sum_{\alpha=1}^N \frac{m\tau_0\dot{\gamma}_0}{m+1} \left(\frac{\dot{\gamma}^\alpha}{\dot{\gamma}_0}\right)^{\frac{m+1}{m}} & \dot{\gamma}^\alpha \geq 0 \\ +\infty & \dot{\gamma}^\alpha < 0 \end{cases} \quad (49)$$

The proposed SL update has been used in the simulation of copper single crystal response to quasi-static axial loading applied in the highly symmetrical orientations [111] and [001]. All constants have been obtained from the literature [4], see Table I for a summary of the model constants and their values. Simulations considered one material point, where the zero lateral-force condition is enforced by Newton-Raphson iterations involving the SL update tangents. Figure 4 shows the stress-strain curves from simulations and experimental results [26]. In these cases, the performance of the SL update has been compared to a truncated Taylor series expansion of the exponential mapping [8]. For the increment size considered here (simulations with 125 and 230 steps for a total axial strain of 16% have been used for benchmarking), between four and eight terms in the series expansion suffice to reach machine precision. Despite the advantageous conditions for this approximate exponential mapping, linked to the use of relatively small increments to handle the complex hardening

behavior, the overall speedup offered by the SL update with respect to the exponential update is still of a factor of about 3.

We end this section by noting that the proposed update has been successfully employed not only in the solution of material point simulations but also in the simulation of medium-scale finite-element models for the strengthening and hardening size effect in micropillars [27] using multiscale strain-gradient plasticity formulations [28].

4. DISCUSSION

Inspired on differential manifold concepts, we have introduced the SL update: an update for the numerical integration of generalized isochoric flow rules that exactly preserves the plastic incompressibility condition while being consistent with the governing differential equation. By way of numerical examples, we have demonstrated that the SL update results in computing times that are several times smaller than the exponential mapping update evaluated using spectral expansion. The reduction in computing time is further improved for the case of the first and second linearizations, in which the SL update takes an order of magnitude less than the exponential mapping. These dramatic speedups make the SL update an excellent and efficient candidate for large-scale simulations where the constitutive update and its tangents are needed.

The exponential mapping update has been the gold standard in finite-deformation incompressible plasticity simulations for the last 20 years. It is worth remarking that the popularity of the exponential mapping relies on two main features, namely, its ability to preserve the incompressibility condition and its consistency with the flow rule. The latter condition is necessary for guaranteeing the convergence of the update. It should be noted that such properties of the exponential mapping rely heavily on the precision of its calculation, whether it be by means of Taylor truncated series or spectral expansion, are therefore subject to constant monitoring of the error. The SL update presents the advantage that the incompressibility condition will be always exactly satisfied, up to machine precision, and will not depend on error tolerances.

It bears emphasis that the exponential mapping, though extensively employed in incompressible plasticity, is not the exact solution to the flow rule (21), with the sole exception of the case where the slip rate is constant for all systems. For all other cases, it can be shown that the exponential mapping is only first-order accurate, see Appendix A. In the general case of manifold updates, it can be shown that by construction they are, at least, first-order accurate, see Appendix A. In particular, the proposed SL update is first-order accurate. Therefore, from the standpoint of accuracy, the exponential mapping update does not necessarily result in better approximations than the proposed SL update.

We end by noting that the particular choice of the embedding and submersion mappings adopted in this work leads to an expression of the SL update, (32), that may be found in Hairer *et al.* [16, Chapter IV, Example 4.6] in the context of projection methods for the numerical solution of volume-invariant Lagrangian dynamics. Hairer and co-workers [16] point out that projection methods, when applied to the time integration of dynamical systems, may break intrinsic symmetries even when the approximation scheme preserves the volume constraint. However, it should be noted that such issues mainly concern the long-time behavior of the dynamical system. We plan to further study such issues in the future for the proposed flow-rule update.

APPENDIX A: ACCURACY ANALYSIS OF MANIFOLD UPDATES AND THE EXPONENTIAL MAPPING

Consider the manifold rate problem given by (9). Let $[t_k, t_{k+1}] \in \mathbb{R}$ be the interval of interest, and let $\Delta t = t_{k+1} - t_k$. By construction, a manifold update $\text{upd}_{x^k} : T_{x^k} M \rightarrow M$ satisfies the consistency conditions (8), and thus, (11) holds for any embedding f and submersion g mappings chosen. Let $\mathbf{x}(t)$ be the solution to the manifold rate problem (9). Then, the local truncation error τ_{k+1} is defined from the expression

$$\mathbf{x}(t_k + \Delta t) = \mathbf{x}(t_k) + \text{upd}_{x(t_k)}(u(x(t_k))) + \Delta t \tau_{k+1}(\Delta t^P), \quad (\text{A.1})$$

where p is the order of accuracy of the update. Using (11), a Taylor expansion of the manifold update around t_k takes the form,

$$\text{upd}_{x_k}(\Delta t \mathbf{u}_k) = \mathbf{x}_k + \Delta t \mathbf{u}_k + O(\Delta t^2).$$

The Taylor expansion of the integral curve reads

$$\begin{aligned} \mathbf{x}(t_k + \Delta t) &= \mathbf{x}(t_k) + \Delta t \dot{\mathbf{x}}(t_k) + O(\Delta t^2) \\ &= \mathbf{x}(t_k) + \Delta t \mathbf{u}(\mathbf{x}(t_k)) + O(\Delta t^2) \\ &= \mathbf{x}(t_k) + \text{upd}_{x(t_k)}(\Delta t \mathbf{u}(\mathbf{x}(t_k))) + O(\Delta t^2). \end{aligned}$$

Then, it follows that the local truncation error is $O(\Delta t)$, and thus, the class of manifold updates presented in this work is at least first-order accurate, that is, $p = 1$. A more detailed analysis considering the particular embedding and submersion mappings may lead to a higher order of accuracy.

We now consider the specific case of the isochoric flow rule,

$$\dot{\mathbf{F}}^p = \dot{\xi} \mathbf{M} \mathbf{F}^p \quad (\text{A.2})$$

where $\mathbf{F}^p(t) \in SL(3)$. The exponential mapping update traditionally used for the numerical integration of (A.2) takes the form

$$\mathbf{F}_{k+1}^p = \exp(\dot{\xi} \mathbf{M} \Delta t) \mathbf{F}_k^p, \quad (\text{A.3})$$

which can be expanded in an absolutely convergent Taylor series as

$$\mathbf{F}_{k+1}^p = \mathbf{F}_k^p + \dot{\xi} \mathbf{M} \mathbf{F}_k^p \Delta t + \frac{1}{2} (\dot{\xi} \mathbf{M})^2 \mathbf{F}_k^p \Delta t^2 + O(\Delta t^3) \quad (\text{A.4})$$

Direct differentiation with respect to time of (A.2) allow us to write

$$\ddot{\mathbf{F}}^p = \{\ddot{\xi} \mathbf{M} + (\dot{\xi} \mathbf{M})^2\} \mathbf{F}^p. \quad (\text{A.5})$$

In view of (A.2) and (A.5), we can write the Taylor expansion of $\mathbf{F}^p(t)$ about t_k as

$$\mathbf{F}^p(t_k + \Delta t) = \mathbf{F}^p(t_k) + \{\dot{\xi} \mathbf{M} \mathbf{F}^p\} \Big|_{t_k} \Delta t + \frac{1}{2} \{(\ddot{\xi} \mathbf{M} + (\dot{\xi} \mathbf{M})^2) \mathbf{F}^p\} \Big|_{t_k} \Delta t^2 + O(\Delta t^3). \quad (\text{A.6})$$

From (A.4) into (A.6), we conclude that $\tau_{k+1}(\Delta t) = \frac{1}{2} \{(\ddot{\xi} \mathbf{M} \mathbf{F}^p)\} \Big|_{t_k} \Delta t$, and therefore, the exponential mapping is first-order accurate.

APPENDIX B: SPECIAL-LINEAR SUBMERSION MAPPING AND ITS TANGENTS

Let $GL(3) = \{\mathbf{F} \in \mathbb{R}^{3 \times 3} \mid \det \mathbf{F} \neq 0\}$ be the general linear group and $SL(3) = \{\mathbf{F} \in \mathbb{R}^{3 \times 3} \mid \det \mathbf{F} = 1\}$ be the SL group, such that $SL(3) \subset GL(3)$. Consider the mapping $g : GL(3) \rightarrow SL(3)$ defined by

$$g(\mathbf{F}) = (\det \mathbf{F})^{-\frac{1}{3}} \mathbf{F} \quad (\text{B.1})$$

or in component notation

$$g_{iJ}(\mathbf{F}) = (\det \mathbf{F})^{-\frac{1}{3}} F_{iJ} \quad (\text{B.2})$$

Moreover, recall the identities

$$\begin{aligned} \frac{\partial \det \mathbf{F}}{\partial F_{iJ}} &= \text{adj}(\mathbf{F})_{iJ} = \det(\mathbf{F}) F_{Ji}^{-1} \\ \frac{\partial F_{Ji}^{-1}}{\partial F_{kL}} &= -F_{Jk}^{-1} F_{Li}^{-1} \end{aligned}$$

Then, the components of the first tangent $T_{\mathbf{F}}g$ take the form

$$(T_{\mathbf{F}}g)_{iJkL} \equiv \frac{\partial g_{iJ}(\mathbf{F})}{\partial F_{kL}} = (\det \mathbf{F})^{-\frac{1}{3}} \left\{ \delta_{ik} \delta_{JL} - \frac{1}{3} F_{Lk}^{-1} F_{iJ} \right\} = (\det \mathbf{F})^{-\frac{1}{3}} \delta_{ik} \delta_{JL} - \frac{1}{3} F_{Lk}^{-1} g_{iJ}(\mathbf{F}), \quad (\text{B.3})$$

and the second tangent components are given by

$$\begin{aligned} (T_{\mathbf{F}}^2 g)_{iJkLpQ} &\equiv \frac{\partial^2 g_{iJ}(\mathbf{F})}{\partial F_{pQ} \partial F_{kL}} = -\frac{1}{3} \left\{ (\det \mathbf{F})^{-\frac{1}{3}} F_{Qp}^{-1} \delta_{ik} \delta_{JL} - F_{Lp}^{-1} F_{Qk}^{-1} g_{iJ}(\mathbf{F}) + F_{Lk}^{-1} \frac{\partial g_{iJ}(\mathbf{F})}{\partial F_{pQ}} \right\} \\ &= -\frac{1}{3} (\det \mathbf{F})^{-\frac{1}{3}} \left\{ F_{Qp}^{-1} \delta_{ik} \delta_{JL} + F_{Lk}^{-1} \delta_{ip} \delta_{JQ} - \left(F_{Lp}^{-1} F_{Qk}^{-1} + \frac{1}{3} F_{Lk}^{-1} F_{Qp}^{-1} \right) F_{iJ} \right\}. \end{aligned} \quad (\text{B.4})$$

We now show that the mapping (B.1) is a submersion. The manifolds $GL(3)$ and $SL(3)$ are particular cases of Lie groups, and therefore, an entire atlas can be constructed using any local chart. It follows that all manifolds operations on arbitrary points can be referred to operations on the identity element (matrix) $\mathbf{I} \in GL(3)$ using left and right translations, see [17]. Thus, it suffices to show that the map g is a submersion at the identity element. We identify the tangent spaces at the identity $gl(3) = T_{\mathbf{I}}GL(3) = \{\mathbf{U} \in \mathbb{R}^{3 \times 3}\}$ and $sl(3) = T_{\mathbf{I}}SL(3) = \{\mathbf{V} \in \mathbb{R}^{3 \times 3} : \text{trace} \mathbf{V} = 0\}$, also known as the *Lie algebras* of the Lie groups $GL(3)$ and $SL(3)$, respectively. We further note that $sl(3) \subset gl(3)$. Then, for any $\mathbf{V} \in sl(3)$, choose $\mathbf{U} = \mathbf{V}$, and note that

$$\begin{aligned} T_{\mathbf{I}}g \cdot \mathbf{U} &= \mathbf{U} - \frac{1}{3} \text{trace}(\mathbf{U}) \mathbf{I} \\ &= \mathbf{V}. \end{aligned}$$

Thus, $T_{\mathbf{F}}g$ is onto $T_{\mathbf{F}}SL(3) \forall \mathbf{F} \in GL(3)$, and therefore, g is a submersion.

ACKNOWLEDGEMENTS

The authors gratefully acknowledge the support of the US Department of Energy National Nuclear Security Administration through Caltech's PSAAP Center for the Predictive Modeling and Simulation of High-Energy Density Dynamic Response of Materials under Award Number DE-FC52-08NA28613. DH also acknowledges the financial support of Conicyt Chile through their science and technology graduate fellowship.

REFERENCES

1. Weber G, Anand L. Finite deformation constitutive-equations and a time integration procedure for isotropic, hyperelastic viscoplastic solids. *Computer Methods in Applied Mechanics and Engineering* 1990; **79**(2):173–202.
2. Eterovic AL, Bathe K-j. A hyperelastic-based large strain elasto-plastic constitutive formulation with combined isotropic-kinematic hardening using the logarithmic stress and strain measures. *International Journal for Numerical Methods in Engineering* 1990; **30**:1099–1114.
3. Simo JC. Algorithms for static and dynamic multiplicative plasticity that preserve the classical return mapping schemes of the infinitesimal theory. *Computer Methods in Applied Mechanics and Engineering* 1992; **99**(1):61–112.
4. Cuitiño AM, Ortiz M. Computational modelling of single crystals. *Modelling and Simulation in Materials Science and Engineering* 1993; **79**(3):160–6.
5. Miehe C. Exponential map algorithm for stress updates in anisotropic multiplicative elastoplasticity for single crystals. *International Journal for Numerical Methods in Engineering* 1996; **39**(19):3367–3390.
6. Anand L, Kothari M. A computational procedure for rate-independent crystal plasticity. *Journal of the Mechanics and Physics of Solids* 1996; **44**:525–558.
7. Moler C, Van Loan C. Nineteen Dubious ways to compute the exponential of a matrix. *SIAM Review* 1978; **20**(4):801–836.
8. Ortiz M, Radovitzky R, Repetto EA. The computation of the exponential and logarithmic mappings and their first and second linearizations. *International Journal for Numerical Methods in Engineering* 2001; **52**(12):1431–1441.
9. Baaser H. The Padé approximation for matrix exponentials applied to an integration algorithm preserving plastic incompressibility. *Computational Mechanics* 2004; **34**(3):237–245.
10. Miehe C. Multisurface thermoplasticity for single crystals at large strains in terms of Eulerian vector updates. *International Journal of Solids and Structures* 1996; **33**:3103–3130.

11. Terada K, Watanabe I. Computational aspects of tangent moduli tensors in rate-independent crystal elastoplasticity. *Computational Mechanics* 2007; **40**(3):497–511.
12. Steinmann P, Stein E. On the numerical treatment and analysis of finite deformation ductile single crystal plasticity. *Computer Methods in Applied Mechanics and Engineering* 1996; **129**(3):235–254.
13. Bourbaki N. *Lie Groups and Lie Algebras*, Elements of Mathematics, Vol. VIII. Springer-Verlag: Berlin Heidelberg, 2005.
14. Crouch PE, Grossman R. Numerical integration of ordinary differential equations on manifolds. *Journal of Nonlinear Science* 1993; **3**:1–33.
15. Hairer E. Geometric integration of ordinary differential equations on manifolds. *BIT Numerical Mathematics* 2001; **41**(5):996–1007.
16. Hairer E, Lubich C, Wanner G. *Geometric Numerical Integration. Structure-Preserving Algorithms for Ordinary Differential Equations*. Springer-Verlag: Berlin Heidelberg, 2006.
17. Marsden JE, Ratiu T, Abraham R. *Manifolds, Tensor Analysis, and Applications*, 3rd edition. Springer-Verlag: New York, 2001.
18. Lubliner J. *Plasticity Theory*. Dover Publications Inc.: New York, 1990.
19. Asaro RJ, Lubarda VA. *Mechanics of Solids and Materials*. Cambridge University Press: New York, 2006.
20. Lee EH. Elastic-plastic deformation at finite strains. *Journal of Applied Mechanics* 1969; **36**(1):1–6.
21. Teodosiu C. A dynamic theory of dislocations and its applications to the theory of the elastic-plastic continuum. In *Proceedings of the Conference on Fundamental Aspects of Dislocation Theory*, Vol. 2, Simmons JA (ed.). Natl. Bureau of Standards Special Publication: Washington, 1969; 837–876.
22. Rice JR. Inelastic constitutive relations for solids: an internal-variable theory and its application to metal plasticity. *Journal of the Mechanics and Physics of Solids* 1971; **19**(6):433–455.
23. Lubliner J. On the thermodynamic foundations of non-linear solid mechanics. *International Journal of Non-Linear Mechanics* 1972; **7**(3):237–254.
24. Ortiz M, Stainier L. The variational formulation of viscoplastic constitutive updates. *Computer Methods in Applied Mechanics and Engineering* 1999; **171**:419–444.
25. Franciosi P, Zaoui A. Multislip in fcc crystals a theoretical approach compared with experimental data. *Acta Metallurgica* 1982; **30**(8):1627–1637.
26. Franciosi P. The concepts of latent hardening and strain hardening in metallic single crystals. *Acta Metallurgica* 1985; **33**(9):1601–1612.
27. Hurtado DE, Ortiz M. Surface effects and the size-dependent hardening and strengthening of nickel micropillars. *Journal of the Mechanics and Physics of Solids* 2012; **60**(8):1432–1446.
28. Hurtado DE, Ortiz M. Finite element analysis of geometrically necessary dislocations in crystal plasticity. *International Journal for Numerical Methods in Engineering* 2013; **93**(1):66–79.